Synthesis of Quarter-Wave Coupled Junction Circulators with Degrees 1 and 2 Complex Gyrator Circuits

JOSEPH HELSZAJN, MEMBER, IEEE

Abstract — **The complex gyrator immittance of circulators for which the in-phase eigennetwork is commensurate with those of the degenerate counter-rotating ones, and which may be idealized by a frequency-independent open- or short-circuited boundary condition, may be realized as a 1-port STUB-resistor network of degree 1. If the frequency variation of this eigennetwork cannot be neglected compared to those of the other two, the gyrator circuit is of degree 2. There are altogether eight possible complex gyrator circuits, each of which explicitly exhibits the eigennetworks of the device. A knowledge of that, applicable in any given situation, is mandatory for design.**

I. Introduction

THE CONSTRUCTION OF the 3-port circulator involves the adjustment of one in-phase and two split counter-rotating eigennetworks [1]. The in-phase eigennetwork may be commensurate with those of the demagnetized ones [2] or it may coincide with the frequency at which the split eigennetworks exhibit complex conjugate immittances [3], or it may, in general, be noncommensurate. If it is idealized by a frequency-independent open- or short-circuited boundary condition, then the 1-port complex gyrator immittance of the junction is a STUB R-circuit of degree 1, otherwise it is a STUB R-circuit of degree 2. Although the degenerate counter-rotating eigennetworks usually exhibit an open-circuited wall at the terminals of the junction, they may, strictly speaking, also exhibit a short-circuited wall there, so that it is in fact possible to realize four 1-port gyrator circuits for each class of solution. The main purpose of this paper is to summarize the four possible complex gyrator networks of each degree and to form the network problem for the degree 2 topologies. A knowledge of the appropriate eigennetworks and complex gyrator circuit in any given situation is, of course, an essential prerequisite for design. The 1-port complex gyrator circuits of degree 2, interestingly enough, explicitly exhibit both the in-phase and split counter-rotating eigennetworks of the magnetized junction and thus permit the synthesis problem to be directly posed in terms of the microwave problem. This network has been specifically drawn in [4]–[11]. A host of equivalent circuits have been proposed over the years for the classic 3-port junction circulator, and some of these are described in [12]–[21], [28].

Manuscript received June 20, 1984; revised January 4, 1985.

The author is with the Department of Electrical and Electronic Engineering, Heriot-Watt University, Edinburgh EH1 1HT, Scotland.

II. Complex Gyrator Circuits of Degrees 1 and 2 of Junction Circulators with Open- and Short-Circuited In-Phase Eigennetworks

The eigenvalue diagrams employed to classify the 1-port complex gyrator circuits of weakly magnetized junction circulators usually assume that the demagnetized counter-rotating ($S^{\pm}$) and in-phase (S^0) eigenvalues are $S^{\pm}=1$ and $S^0=\pm 1$ [1], [5], [7], [21]. However, these two solutions do not form a full set since it is also possible to have $S^{\pm}=-1$ and $S^0=\pm 1$. Fig. 1 depicts the complete family of solutions. The in-phase and counter-rotating eigenvalues are the reflection variables of 1-port reactive networks known as the eigennetworks of the junction. These may be realized in terms of the poles of the eigenvalues in either a first or second Foster form, in the manner illustrated in Fig. 2(a) and (b) [3]. Counter-rotating poles, in this expansion, that have the symmetry of the junction are associated with the in-phase eigennetwork. Whether a pole of an eigenvalue exhibits an electric or magnetic wall at the symmetry plane is readily established by application of the appropriate in-phase or counter-rotating eigenvectors at the terminals of the junction [1], [27]. Although the lowest order in-phase pole is usually associated with a magnetic-wall boundary condition at the symmetry plane of the junction, it may also exhibit an electric wall there, as, for instance, in an E-plane junction, or if a thin metal wall is introduced through the plane of symmetry of an H-plane one, or in the vicinity of the counter-rotating poles having the symmetry of the junction. Likewise, although the lowest order counter-rotating poles of the junction are usually associated with electric-wall boundary conditions at the symmetry plane of the junction, they may still exhibit magnetic-wall boundary conditions at its terminals by realizing the eigennetworks by half-wave-long transmission lines instead of quarter-wave ones. Fig. 3 illustrates the distinction between the in-phase eigennetworks for E- and H-plane junctions.

Substitution of an electric wall for a magnetic one, for either of the eigenvalues, leads to a reversal in the direction of circulation of the junction, as is readily verified if the splitting between the eigenvalues is correctly reset [26]. This is also the case if $S^{\pm}$ are interchanged. The open-circuit parameters of the junction do not exist if the in-phase

0018-9480/85/0500-0381$01.00

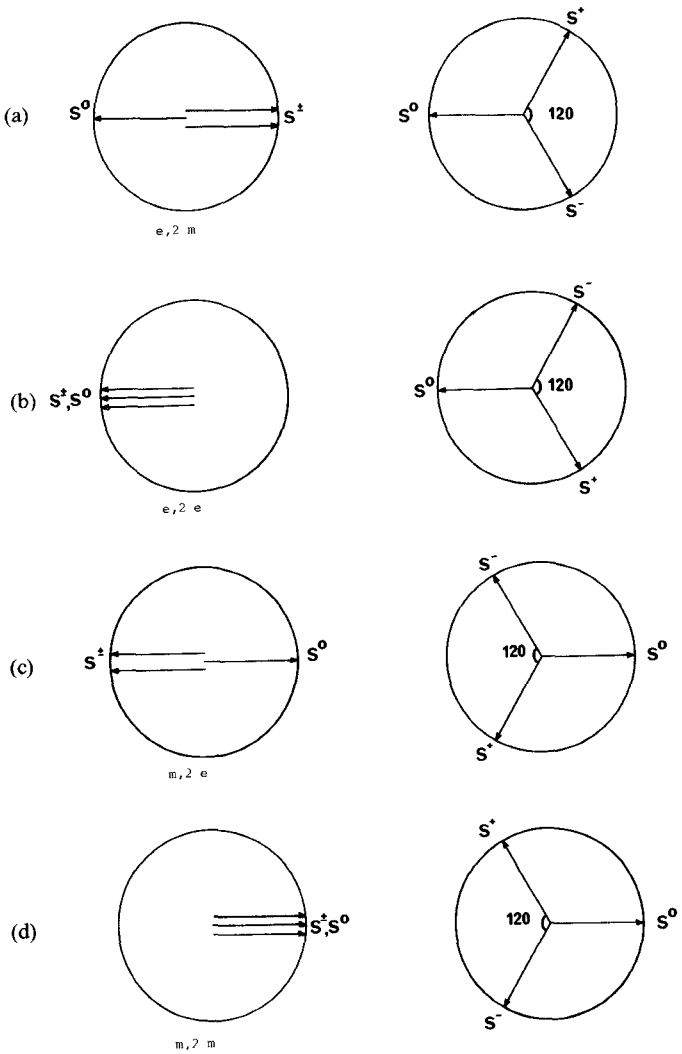

Fig. 1. (a) First and second circulation adjustments for junction circulator with $S^0 = -1$ and $S^{\pm} = 1$. (b) First and second circulation adjustments for junction circulator with $S^0 = -1$ and $S^{\pm} = -1$. (c) First and second circulation adjustments for junction circulator with $S^0 = 1$ and $S^{\pm} = -1$. (d) First and second circulation adjustments for junction circulator with $S^0 = 1$ and $S^{\pm} = 1$.

eigennetwork exhibits a magnetic-wall boundary condition, and conversely the short-circuit parameters do not exist if it exhibits an electric-wall boundary condition. If the in-phase and degenerate eigennetworks exhibit dual walls, then the demagnetized junctions have neither open- nor short-circuited parameters. If the in-phase eigennetwork is idealized by a frequency-independent electric or magnetic wall at the terminals of the junction then the corresponding eigenvalue diagram is of degree 1, otherwise it is of degree 2. A number of practical examples of the latter class have been mentioned in [4], [7], [10], [11].

The eigenvalue diagrams in Fig. 1(a)–(d) may be labelled according to whether the eigennetworks exhibit electric or magnetic walls at the terminals of the junction and according to whether the in-phase eigennetwork is idealized by a frequency-independent electric or magnetic wall or not as $e,2m$, $e,2e$, $m,2e$, and $m,2m$ of degree 1 or 2. If the in-phase eigennetwork is idealized by either a frequency-independent open- or short-circuited stub at the terminals of the junction, then the 1-port complex gyrator circuit is a

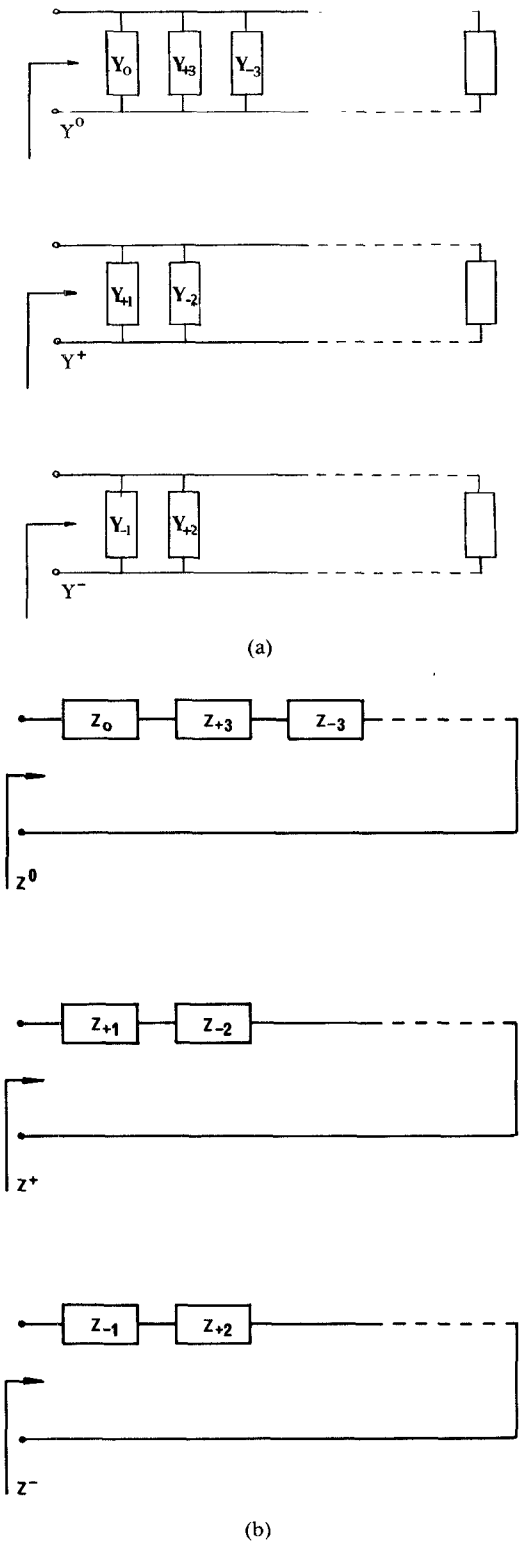

Fig. 2. First and second foster forms of in-phase and counter-rotating eigennetworks of junction circulator.

STUB-R load of degree 1, otherwise it is a STUB-R load of degree 2. The 1-port gyrator circuits of degrees 1 and 2 discussed here are formed in terms of the in-phase (Z^0, Y^0) and counter-rotating $(Z^{\pm}, Y^{\pm})$ immittance eigenvalues; both the in-phase and counter-rotating eigennetworks are explicitly exhibited by the gyrator circuits of degree 2.

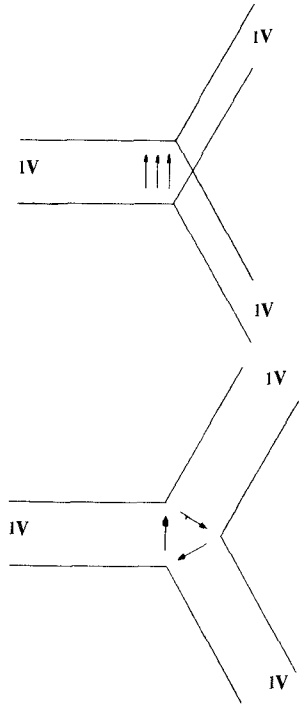

Fig. 3. In-phase excitation of E- and H-plane junctions.

The complex gyrator circuits of degree 1, obtained by idealizing the in-phase eigennetwork by a frequency-independent electric wall and those of the degenerate counter-rotating ones by either magnetic or electric walls will now be examined as a preamble to summarizing the dual problem for which the in-phase eigennetwork exhibits a magnetic wall at the terminals of the network. Fig. 4 gives the complex gyrator circuits for the four degree 1 situations, and Fig. 5 illustrates the corresponding lumped-element circuits. Since the short-circuit parameters do not in the former instance exist, the derivation starts by forming the classic gyrator 1-port impedance in terms of the open-circuit parameters of the junction with $V_3 = I_3 = 0$

$$Z_{in} = Z_{11} - \frac{Z_{12}^2}{Z_{13}}. \tag{1}$$

The short-circuit parameters Z_{11}, Z_{12}, and Z_{13} are given in the usual way in terms of the admittance eigenvalues Z^0 and $Z^{\pm}$ by

$$Z_{11} = \frac{Z^0 + Z^+ + Z^-}{3} \tag{2}$$

$$Z_{12} = \frac{Z^0 + Z^+ \exp(j120) + Z^- \exp(-j120)}{3} \tag{3}$$

$$Z_{13} = \frac{Z^0 + Z^+ \exp(-j120) + Z^- \exp(j120)}{3}. \tag{4}$$

Exact complex gyrator circuits of degree 1 may now be formed at the frequencies at which the counter-rotating eigennetworks exhibit either electric or magnetic walls.

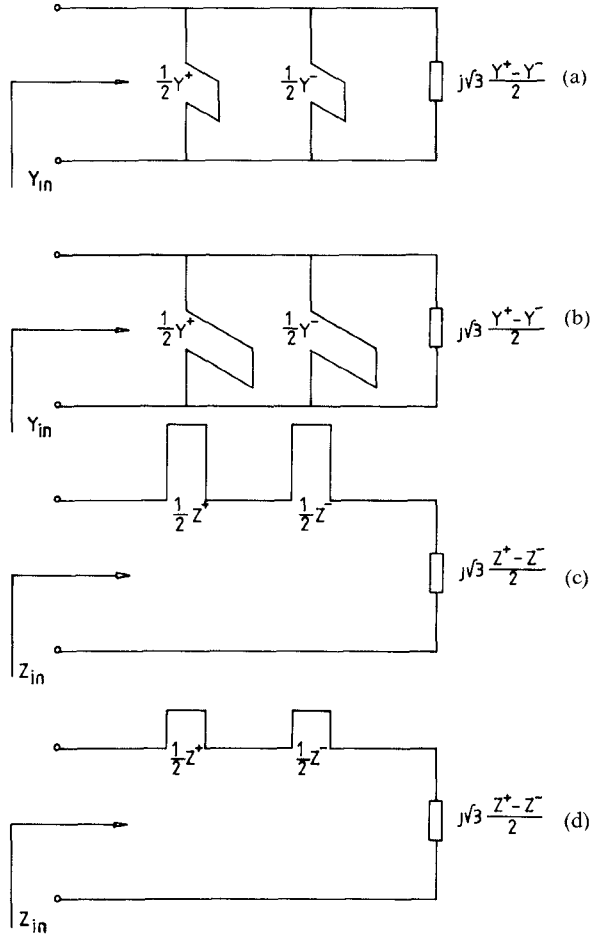

Fig. 4. Complex gyrator circuits of degree 1.

Idealizing the in-phase eigennetwork by an electric wall gives

$$Z^0 = 0. \tag{5}$$

The result is

$$Y_{in} = \frac{1}{Z_{in}} = \frac{(Y^+ + Y^-)}{2} - j\sqrt{3}\,\frac{(Y^+ - Y^-)}{2}. \tag{6}$$

This result has historically been given with an approximation sign but is exact as can be readily verified by tracing (1) and (6). The case where the degenerate eigenvalues exhibit magnetic walls may now be distinguished from that for which they have electric walls. In the first situation, the counter-rotating eigennetworks may be realized using quarter-wave-long short-circuited stubs, and the complex gyrator circuit takes the form in Fig. 4(a). In the second case, the counter-rotating networks may be realized by half-wave-long short-circuited stubs, and the corresponding complex gyrator circuit has the topology indicated in Fig. 4(b). The counter-rotating eigenvalues are also, in this latter instance, interchanged on the eigenvalue diagram so that the junction now circulates in the opposite direction.

Some additional distinguishable properties of these two solutions are that for the eigenvalue diagram in Fig. 1(a) the real part of the gyrator immittance tends to a magnetic wall as the junction is demagnetized, while that in Fig. 1(b)

tends to an electric wall under the same condition. Whether one or the other situation applies is determined by whether the degenerate eigennetworks have magnetic or electric walls. Furthermore, the required angular splitting on the eigenvalue diagram is in the former case, half that of the latter one. Surprisingly enough, the susceptance slope parameter of the second solution is now a function of the splitting. All of these aspects may be readily verified by scrutinizing Figs. 1(a) and (b) and 4(a) and (b), or they may be more directly demonstrated by assuming that $Y^{\pm}$ in Fig. 2 may phemenologically be written as

$$Y^{\pm} = -ja_1^2 Y_1 \cot(\theta_1 \pm \Delta\theta_1). \tag{7}$$

θ_1 is the electrical length of the degenerate counter-rotating eigennetworks, $\pm\Delta\theta_1$ represents the perturbation in the demagnetized eigennetworks when the junction is magnetized, Y_1 is the characteristic admittance of the eigennetworks which, for simplicity, are assumed to coincide with those of the demagnetized junction, and a_1 is the turns ratio of an ideal transformer that represents the coupling between the three transmission lines and the resonator.

Forming (6) in the vicinities of $\theta_1 = \pi/2$ and π readily yields

$$Y_{\text{in}} \approx \sqrt{3} a_1^2 Y_1 \tan\Delta\theta_1 - ja_1^2 Y_1 \frac{\cot\theta_1(1+\tan^2\Delta\theta_1)}{1-\cot^2\theta_1 \tan^2\Delta\theta_1} \tag{8}$$

$$Y_{\text{in}} \approx -\sqrt{3} a_1^2 Y_1 \cot\Delta\theta_1 - ja_1^2 Y_1 \frac{\tan\theta_1(1+\tan^2\Delta\theta_1)}{\tan^2\theta_1 - \tan^2\Delta\theta_1}. \tag{9}$$

The real part of the first solution is asymptotic to a magnetic wall in the neighborhood of $\pi/2$ as the junction is demagnetized and the second one to an electric wall in the vicinity of $\theta_1 = \pi$ under the same conditions. The imaginary part of the second solution also differs from the first one in that it exhibits a passband at

$$\tan\theta_1 = 0 \tag{10}$$

and stopbands at

$$\tan\theta_1 = \pm\tan\Delta\theta_1 \tag{11}$$

and that in the vicinity of $\theta_1 = \pi$ its susceptance is dependent upon $\Delta\theta_1$. These features may also be appreciated by inspection of the lumped-element gyrator circuits in Fig. 5. The susceptance slope parameters of these two arrangements, neglecting the frequency variation of the denominator polynomials, are given by (8) and (9) in the vicinities of $\theta_1 = \pi/2$ and π as

$$B' \approx \frac{\pi}{4} a_1^2 Y_1 \tag{12}$$

$$B' \approx \frac{\pi}{2} a_1^2 Y_1 / \tan^2\Delta\theta_1 \tag{13}$$

respectively. The loaded Q-factors for these two solutions have both the same form and are indeed identical if B' in (13) is realized with the aid of an open-circuited quarter-wave-long stub instead of a short-circuited half-wave-long one

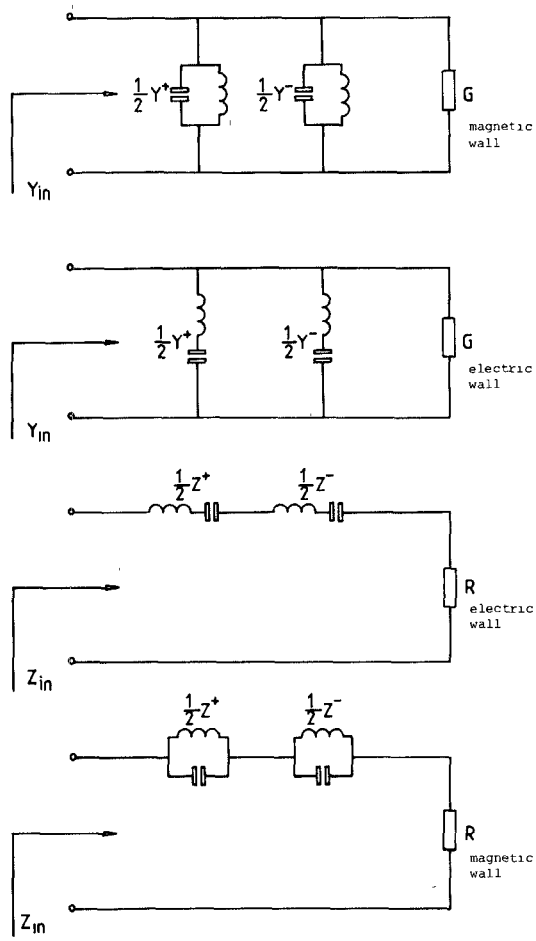

Fig. 5. Lumped-element equivalent circuits of complex gyrator circuits of degree 1.

$$Q_L = \frac{B'}{G_{\text{in}}} = \frac{\pi}{4\sqrt{3}} \cot\Delta\theta_1 \tag{14}$$

$$Q_L = \frac{\pi}{2\sqrt{3}} \cot\Delta\theta_1. \tag{15}$$

$\Delta\theta_1$ is determined by the real parts of (8) and (9). The nature of these two solutions has been verified by forming their exact frequencies responses in the vicinities of $\theta_1 = \pi/2$ and π using (1). The $e,2m$ degree 1 solution described by (8), (12), and (14) is of course a standard result and need not be dwelt on further. Fig. 6 gives the frequency response of one solution for completeness. The $e,2e$ degree 1 result, given by (9), (13), and (15), however, differs from the classic one in that both its susceptance slope parameter and conductance are dependent upon the magnetic variables of the resonator. Figs. 7 and 8 display the frequency responses of this solution for two different arbitrary values of the magnetic parameter. The passbands and stopbands exhibited by (10) and (11) are noted. The fact that the gyrator conductance is negative in this result merely means that the device rotates in the opposite direction from the solution in Fig. 6.

The complex gyrator circuit in Fig. 4(a) is the classic result met in the theory of planar and turnstile H-plane

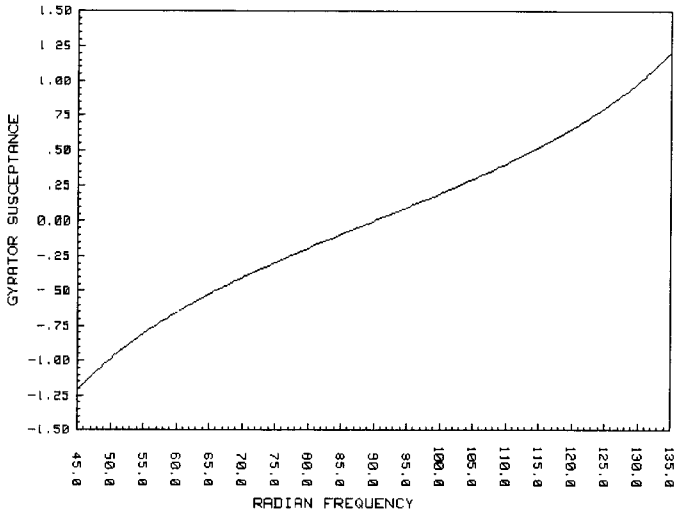

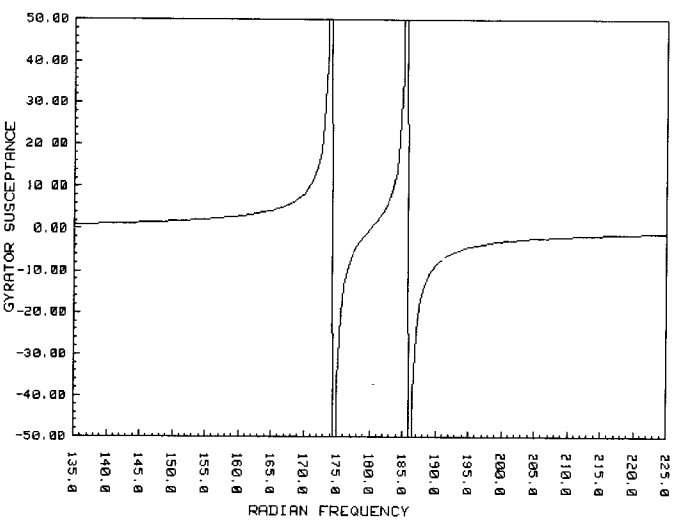

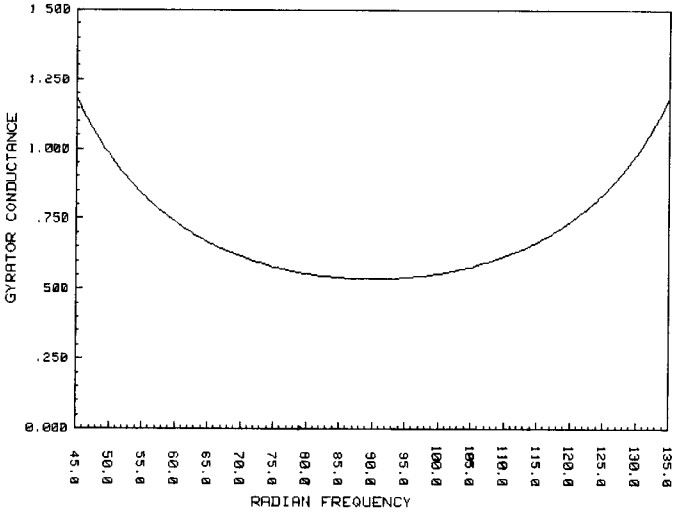

Fig. 6. Conductance and susceptance of $e,2m$ degree 1 complex gyrator circuit for $\Delta\theta_1 = 0.10$ rad ($a_1^2 Y_1 = 1$).

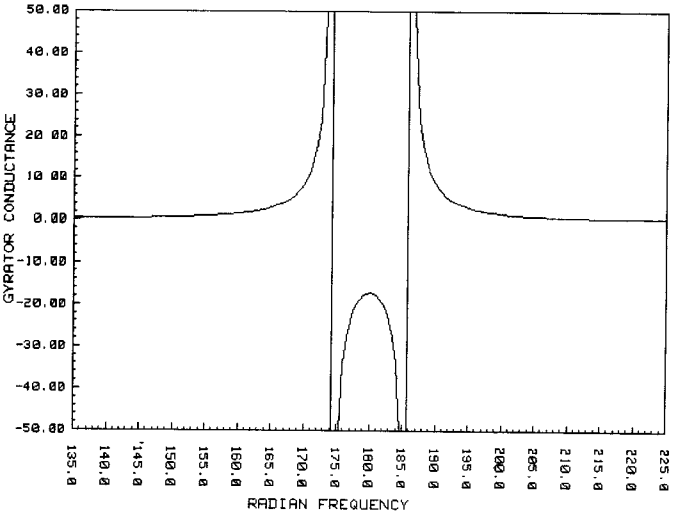

Fig. 7. Conductance and susceptance of $e,2e$ degree 1 complex gyrator circuit for $\Delta\theta_1 = 01.0$ rad ($a_1^2 Y_1 = 1$).

junctions using quarter-wave-long open resonators [12], [27]. The one in Fig. 4(b) may also be realized in an E-plane junction. The demagnetized junction now exhibits a bandstop instead of a bandpass characteristic [15], [20].

The angles $\theta^{\pm}$ on the eigenvalue diagrams are functions of θ_1, $\Delta\theta_1$, and B' and may be formed by constructing the reflection coefficients $S^{\pm} = 1\exp(-j2\theta^{\pm})$.

$$S^{\pm} = \frac{Y_0 - Y^{\pm}}{Y_0 + Y^{\pm}} \tag{16}$$

where Y_0 is the characteristic admittance at the ports.

The derivation of the 1-port complex gyrator circuits of degree 1 for the cases where the in-phase eigennetwork is idealized by a frequency independent magnetic wall and those of the counter-rotating ones by either magnetic or electric walls proceeds in a similar fashion except that short-circuit parameters are employed to form the complex gyrator immittances, and that Y^0 instead of Z^0 is assumed to be zero in the approximation problem

$$Z_{\text{in}} = \frac{(Z^+ + Z^-)}{2} + j\sqrt{3}\,\frac{(Z^+ - Z^-)}{2}. \tag{17}$$

The appropriate equivalent circuits are illustrated in Fig. 4(c) and (d). The gyrator resistance is asymptotic to an electric wall in the first instance and to a magnetic one in the second case. The solution in Fig. 4(c) is well behaved in the vicinity of its midband, but that in Fig. 4(d) exhibits stopbands on either side of its passband and a stopband in its demagnetized state.

Short-circuited in-phase eigennetworks may in practice be realized by introducing a short-circuit boundary condition in the form of a thin metal post through the symmetry axis of an H-plane junction or may be directly exhibited by an E-plane junction or may be formed in the vicinity of a pole having the symmetry of the device. An example of an $m,2e$ eigenvalue diagram or complex gyrator circuit of

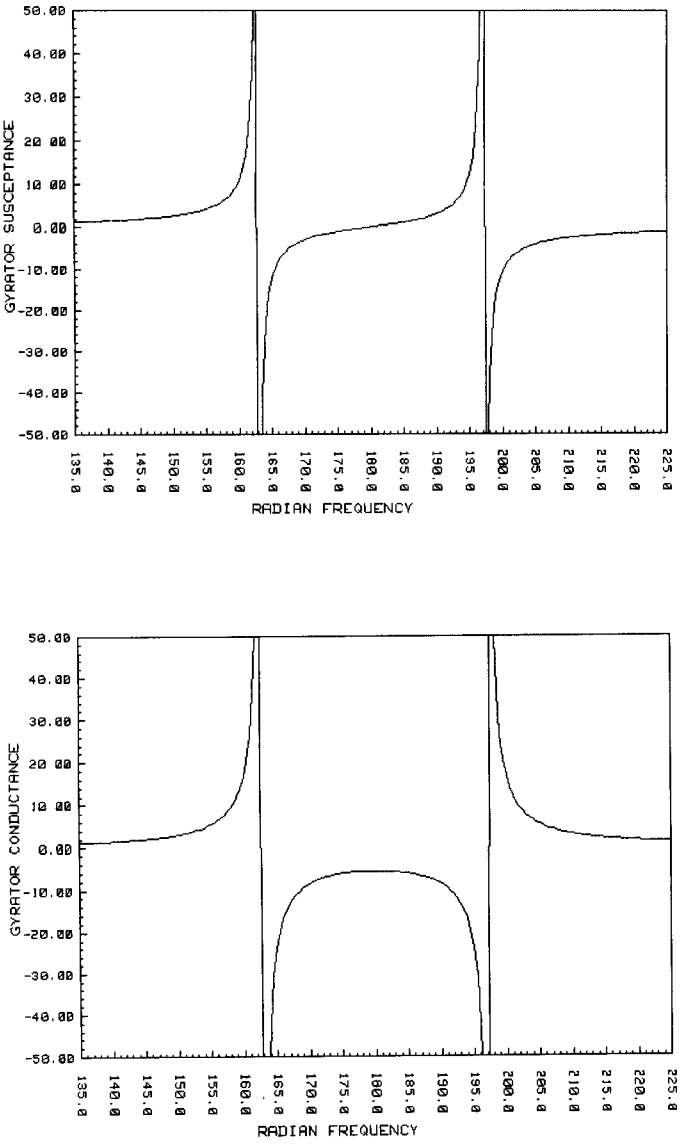

Fig. 8. Conductance and susceptance of $e,2e$ degree 1 complex gyrator circuit for $\Delta\theta_1 = 0.30$ rad ($a_1^2 Y_1 = 1$).

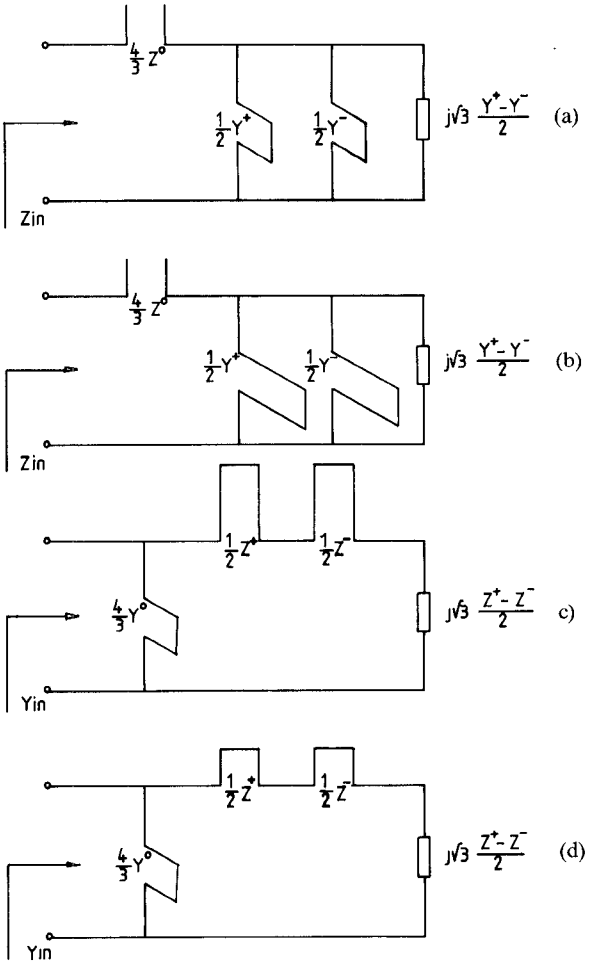

Fig. 9. Complex gyrator circuits of degree 2.

degree 1 may be understood from the situation described in [15]. An example of an $m,2m$ eigenvalue diagram of degree 1 does not come to mind, but a half-wave-long turnstile resonator in an E-plane junction is one possibility.

The derivation of the complex gyrator circuits of degree 2 for the two eigenvalue diagrams in Fig. 1(a) and (b), as well as for the two in Fig. 1(c) and (d), has been outlined in [11] except that the situations for which $S^{\pm} = -1$ are specifically outlined in Fig. 9. It will therefore not be repeated here. Fig. 10 gives the lumped-element equivalent solutions for this class of device. In realizing these circuits, it has been assumed that the real part of the complex gyrator immittance may be formed by idealizing the in-phase eigennetwork by either an electric or magnetic wall [3], [11]. It is readily appreciated that the split shunt parallel and series resonators in Fig. 10 both reduce to single shunt resonators in the vicinities of the passband frequencies, and that, likewise, the series combinations of the series and parallel resonators reduce to series resonators at the same frequencies. Each of the gyrator circuits of degree 2 has the same transmission zeros and thus each can be arranged to exhibit the same transmission characteristic. The insertion-loss function for this class of network is akin to that realizable with a complex gyrator circuit of degree 1 coupled by a single U.E. Examples of this situation have been mentioned in [4], [7], [10], [11]. The synthesis of U.E.-coupled complex gyrator circuits of degree 2 is of course of interest [6], [10] and will be tackled in some detail in the next section. The synthesis of U.E.-coupled gyrator circuits of degree 1 is well rehearsed in the literature [22]–[25].

III. The Network Problem

Since the circuits in Fig. 9(a) and (b) have similar topologies as have those in Fig. 9(c) and (d), the matching problems reduce to the solutions of the two situations in Fig. 11(a) and (b). Furthermore, since all four circuits have the same transmission zeros, they may all be synthesized from the same insertion-loss function. Although the eigennetworks of the junction may consist of half- or three-quarter-wave-long stubs, the circuits in Fig. 11 employ quarter-wave-long stubs to permit exact synthesis of the network problem. The equivalence between the circulator

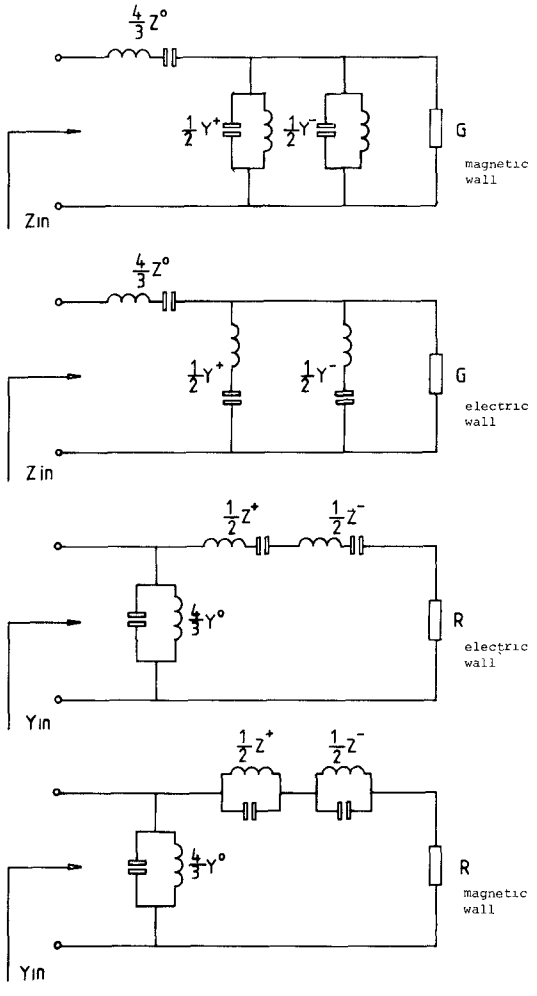

Fig. 10. Lumped-element equivalent circuits of complex gyrator circuits of degree 2.

and network problems is then achieved by equating the susceptance or reactance slope parameters of the two.

The Chebyshev approximation problem may be readily formed from a knowledge of the n-transmission zeros of the transformed variable Z and follows closely the procedure employed in [25]. The appropriate conformal transformation between the Z and Richards S variables is in this instance given by

$$Z^2 = 1 + S^2/\Omega_1^2 \tag{18}$$

where S is

$$S = j \tan\theta \tag{19}$$

and Ω_1 is determined by the lower band-edge electrical length θ_1 indicated in Fig. 12

$$\Omega_1 = j \tan\theta_1. \tag{20}$$

The networks in Fig. 11 have a double-ordered pole at $S = 0$, due to the two stubs

$$Z_{1,2} = 1 \tag{21}$$

and a half-ordered pole at $S = 1$

$$Z_3 = \sqrt{1 + 1/\Omega_1^2} \tag{22}$$

the latter being due to the unit element.

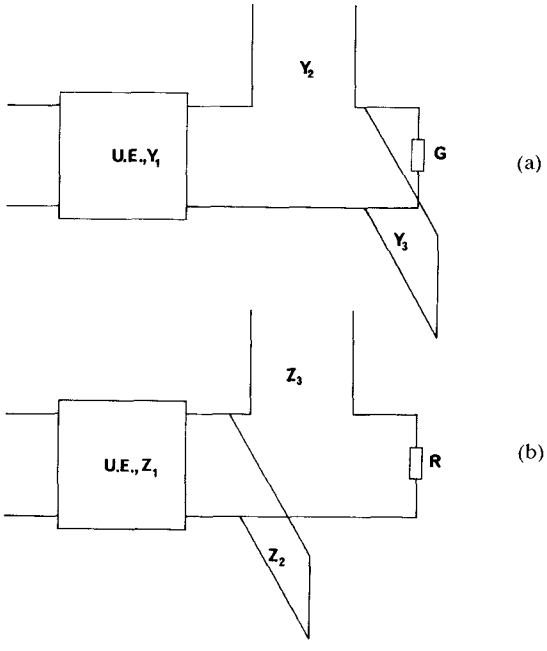

Fig. 11. (a) Quarter-wave coupled shunt STUB-R load of degree 2. (b) Quarter-wave coupled series STUB-R load of degree 2.

The auxiliary function is

$$f(Z) = \prod_{i=1}^{n} \sqrt{\frac{Z_i + Z}{Z_i - Z}} \tag{23}$$

where for the problem at hand

$$\prod_{i=1}^{n} (Z_i + Z) = (1+Z)^2 \left(\sqrt{1 + \frac{1}{\Omega_1^2}} + Z \right). \tag{24}$$

The Chebyshev equiripple insertion-loss function is given in terms of the auxiliary function by

$$L = 1 + K^2 + \epsilon^2 \left[\frac{f(Z) + f(-Z)}{2} \right]^2 \tag{25}$$

or

$$L = 1 + K^2 + \epsilon^2 \left[\frac{(1+Z^2)\sqrt{1 + \frac{1}{\Omega_1^2}} + 2Z^2}{(1-Z^2)\left(1 + \frac{1}{\Omega_1^2} - Z^2\right)^{1/2}} \right]^2. \tag{26}$$

Writing Z in terms of S readily gives the required result

$$L = 1 + K^2 + \epsilon^2 \left[\frac{\left(\sqrt{1+\Omega_1^2} + 2\Omega_1\right)S^2 + 2\Omega_1^2\left(\sqrt{1+\Omega_1^2} + \Omega_1\right)}{S^2\sqrt{1-S^2}} \right]^2. \tag{27}$$

This may be synthesized separately without difficulty to give the circuits indicated in Fig. 11. Some results for the topology in Fig. 11(a) are given in Table I. These tables are also directly applicable to the circuit in Fig. 11(b) by noting the duality between the two circuits. This is done by replacing Y_1 with Z_1, Y_2 with Z_2, Y_3 with Z_3, and G with R.

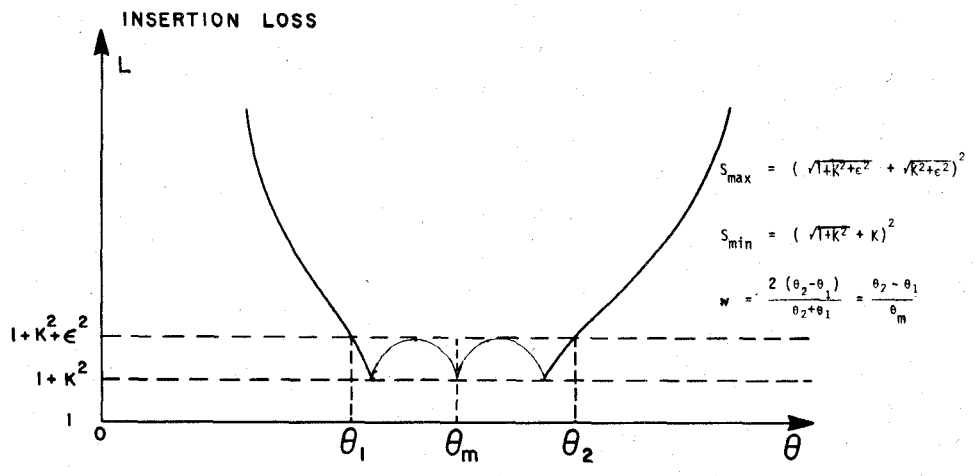

Fig. 12. $n = 3$ equiripple insertion-loss function.

TABLE I

DEGREE N= 3 S(MAX)= 1.15 S(MIN)= 1

W	G	Y3	G	Y1	Y2
0.2000	0.0443	0.2039	3.6140	0.2105	0.0060
0.2500	0.0678	0.2477	2.8708	0.2603	0.0133
0.3000	0.0951	0.2873	2.3716	0.3084	0.0227
0.3500	0.1258	0.3222	2.0120	0.3546	0.0357
0.4000	0.1589	0.3521	1.7397	0.3987	0.0520
0.4500	0.1940	0.3769	1.5256	0.4405	0.0743
0.5000	0.2303	0.3966	1.3524	0.4799	0.1008
0.5500	0.2673	0.4115	1.2089	0.5170	0.1327
0.6000	0.3045	0.4217	1.0877	0.5518	0.1703
0.6667	0.3535	0.4286	0.9523	0.5945	0.2302
0.7000	0.3775	0.4295	0.8935	0.6144	0.2646
0.7500	0.4127	0.4278	0.8141	0.6424	0.3224
0.8000	0.4467	0.4229	0.7435	0.6684	0.3879
0.8500	0.4793	0.4152	0.6804	0.6923	0.4620
0.9000	0.5105	0.4052	0.6233	0.7145	0.5455
0.9500	0.5401	0.3930	0.5715	0.7349	0.6393
1.0000	0.5681	0.3791	0.5241	0.7537	0.7440

DEGREE N= 3 S(MAX)= 1.15 S(MIN)= 1.02

W	G	Y3	G	Y1	Y2
0.2000	0.0468	0.2220	3.7274	0.2185	0.0073
0.2500	0.0715	0.2695	2.9606	0.2700	0.0142
0.3000	0.1002	0.3120	2.4456	0.3197	0.0243
0.3500	0.1323	0.3493	2.0745	0.3673	0.0382
0.4000	0.1669	0.3810	1.7935	0.4126	0.0563
0.4500	0.2033	0.4071	1.5725	0.4554	0.0792
0.5000	0.2409	0.4275	1.3937	0.4957	0.1073
0.5500	0.2790	0.4425	1.2456	0.5335	0.1411
0.6000	0.3172	0.4525	1.1205	0.5688	0.1808
0.6667	0.3672	0.4585	0.9808	0.6120	0.2440
0.7000	0.3916	0.4587	0.9200	0.6320	0.2803
0.7500	0.4272	0.4558	0.8380	0.6601	0.3411
0.8000	0.4614	0.4496	0.7653	0.6861	0.4099
0.8500	0.4942	0.4405	0.7001	0.7100	0.4876
0.9000	0.5252	0.4288	0.6412	0.7319	0.5750
0.9500	0.5546	0.4150	0.5878	0.7521	0.6731
1.0000	0.5823	0.3995	0.5389	0.7707	0.7831

Since the more useful values of loaded Q-factors in junction circulators are obtained by having the gyrator conductance traverse the origin of the Smith Chart, inspection of the tabulated data indicates that not all degree 2 complex gyrator circuits are equally well suited for matching with a single U.E. The realization of the appropriate immittance levels of the gyrator circuits of practical circulators must of course be determined either experimentally or theoretically [27].

IV. Conclusions

Three-port junction circulators employing weakly magnetized resonators may exhibit one of four eigenvalue diagrams of degree 1 or 2. There are, therefore, eight possible complex gyrator circuits and these have been directly realized in terms of the eigennetworks of the junction. A knowledge of that, applicable in any given situation, is essential for design. The topologies of the gyrator circuits derived in this paper are particularly suitable for use in the synthesis problem.

Acknowledgment

The author would like to thank Dr. R. Levy, of MDL, MA, for contributing the network problem.

References

[1] B. A. Auld, "The synthesis of symmetrical waveguide circulator," *IRE Trans. Microwave Theory Tech.*, vol. MTT-7, pp. 238–246, 1959.

[2] U. Milano, J. U. Saunders, and L. E. Davis, Jr., "A Y-junction strip-line circulator," *IRE Trans. Microwave Theory Tech.*, vol. MTT-8, pp. 346–350, May 1960.

[3] J. Helszajn, "Operation of tracking circulator," *IEEE Trans. Microwave Theory Tech.*, vol. MTT-29, pp. 700–707, July 1981.

[4] Y. Konishi, "A high power u.h.f. circulator," *IEEE Trans. Microwave Theory Tech.*, vol. MTT-15, pp. 700–708, Dec. 1967.

[5] J. Helszajn, "Wideband circulator adjustment using $n=1$ and $n=0$ electromagnetic-field patterns," *Electron Lett.*, vol. 6, pp. 729–731, Nov. 1970.

[6] Y. Naito and N. Tanaka, "Broad-banding and changing operation frequency of circulator," *IEEE Trans. Microwave Theory Tech.*, vol. MTT-19, pp. 367–372, Apr. 1971.

[7] J. Helszajn, "Three-resonant mode adjustment of the waveguide circulator," *Radio Electron. Eng.*, vol. 42, pp. 1–4, Apr. 1972.

[8] Y. Akaiwa, "Input impedance of a circulator with an in-phase eigen-excitation resonator," *Electron Lett.*, vol. 9, no. 12, June 1973.

[9] J. Helszajn, "Standing wave solution of planar irregular and hexagonal resonators," *IEEE Trans. Microwave Theory Tech.*, vol. MTT-29, June 1981.

[10] W. S. Piotrowsky and J. E. Raul, "Low-loss broad-band EHF circulators," *IEEE Trans. Microwave Theory Tech.*, vol. MTT-24, pp. 863–866, Nov. 1976.

[11] J. Helszajn, "Complex gyrator circuits of planar circulators using higher order modes in a disk resonator," *IEEE Trans. Microwave Theory Tech.*, vol. MTT-31, pp. 931–937, Nov. 1983.

[12] C. E. Fay and R. L. Comstock, "Operation of the ferrite junction circulator," *IEEE Trans. Microwave Theory Tech.*, vol. MTT-13, pp. 15–27, 1965.

[13] B. L. Humphreys and J. B. Davies, "The synthesis of *n*-port circulators," *IRE Trans. Microwave Theory Tech.*, vol. MTT-10, pp. 551–554, Nov. 1962.
[14] H.-J. Butterweck, "Der *Y*-Zirkulator," *Arch. Elek. Ubertragung.*, vol. 17, pp. 163–176, 1963.
[15] M. Omori, "An improved *E*-plane waveguide circulator," in *G-MTT Int. Microwave Symp. Dig.*, 1968, p. 228.
[16] H. Bosma, "A general model for junction circulators: Choice of magnetization and bias field," *IEEE Trans. Magn.*, vol. MAG-4, pp. 587–596, 1968.
[17] J. O. Bergman and C. Christensen, "Equivalent circuit for a lumped element *Y* circulator," *IEEE Trans. Microwave Theory Tech.*, vol. MTT-16, pp. 308–310, May 1968.
[18] S. J. Salay and H. J. Peppiatt, "An accurate junction circulator design procedure," *IEEE Trans. Microwave Theory Tech.*, vol. MTT-20, pp. 192–193, Feb. 1972.
[19] J. Bittar and J. Verszely, "A general equivalent network of the input impedance of symmetric three-port circulators," *IEEE Trans. Microwave Theory Tech.*, vol. MTT-28, pp. 807–808, July 1980.
[20] K. Solbach, "Equivalent circuit representation for the *E*-plane circulator," *IEEE Trans. Microwave Theory Tech.*, vol. MTT-30, pp. 806–809, 1982.
[21] U. Goebel and C. Schieblich, "A unified equivalent circuit representation of *H* and *E*-plane junction circulators," in *Eur. Microwave Conf.*, 1983, pp. 803–808.
[22] L. K. Anderson, "An analysis of broadband circulators with external tuning elements," *IEEE Trans. Microwave Theory Tech.*, vol. MTT-15, pp. 42–47, Jan. 1967.
[23] J. Helszajn, "The synthesis of quarter-wave coupled circulators with Chebyshev characteristics," *IEEE Trans. Microwave Theory Tech.*, vol. MTT-20, pp. 764–769, Nov. 1972.
[24] R. Levy and J. Helszajn, "Specific equations for one and two section quarter-wave matching networks for stub-resistor loads," *IEEE Trans. Microwave Theory Tech.*, vol. MTT-30, pp. 57–62, Jan. 1982.
[25] R. Levy and J. Helszajn, "Short-line matching networks for circulators and resonant loads," *Inst. Elec. Eng. Proc.*, vol. 130, pt. H, pp. 385–390, Oct. 1983.
[26] R. N. Knerr, C. E. Barnes, and F. Bosch, "A compact broadband thin-film lumped-element *L*-band circulator," *IEEE Trans. Microwave Theory Tech.*, vol. MTT-18, pp. 1100–1108, Dec. 1970.
[27] B. Owen, "The identification of modal resonances in ferrite-loaded waveguide *Y*-junctions and their adjustment for circulation," *Bell Syst. Tech. J.*, vol. 51, pp. 595–627, 1972.
[28] G. Riblet, "The measurement of the equivalent admittance of 3-port circulators via an automated measurement system," *IEEE Trans. Microwave Theory Tech.*, vol. MTT-25, pp. 401–405, May 1977.

Joseph Helszajn (M'64) was born in Brussels, Belgium, in 1934. He received the Full Technological Certificate of the City and Guilds of London Institute from Northern Polytechnic, London, England (1955), the M.S.E.E. degree from the University of Santa Clara, CA (1964), the Ph.D. degree from the University of Leeds, Leeds, England (1969), and the D.Sc. degree from Heriot-Watt University, Edinburgh, Scotland (1976).

He has held a number of positions in the microwave industry. From 1964 to 1966, he was Product Line Manager at Microwave Associates, Inc., Burlington, MA. He is now Professor of Microwave Engineering at Heriot-Watt University. He is the author of the books *Principles of Microwave Ferrite Engineering* (New York: Wiley, 1969), *Nonreciprocal Microwave Junctions and Circulators* (New York: Wiley, 1975), *Passive and Active Microwave Circuits* (New York: Wiley, 1978), and *YIG Resonators and Filters* (New York: Wiley, 1985).

Dr. Helszajn is a Fellow of the Institution of Electronic and Radio Engineers (England) and a Fellow of the Institute of Electrical Engineers. In 1968, he was awarded the Insignia Award of the City and Guilds of London Institute. He is an Honorary Editor of *Microwaves, Antennas and Propagation* (IEE Proceedings).